

CHOROID PLEXUS SEGMENTATION USING OPTIMIZED 3D U-NET

Li Zhao^{}, Xue Feng[†], Craig H. Meyer[†], David C. Alsop[‡]*

^{*}Diagnostic Imaging and Radiology, Children's National Hospital, Washington, DC

[†]Department of Biomedical Engineering, University of Virginia, Charlottesville, VA

[‡]Radiology, Beth Israel Deaconess Medical Center and Harvard Medical School, Boston, MA

ABSTRACT

The choroid plexus is the primary organ that secretes the cerebrospinal fluid. Its structure and function may be associated with the brain drainage pathway and the clearance of amyloid-beta in Alzheimer's Disease. However, choroid plexus segmentation methods have rarely been studied. Therefore, the purpose of this work is to fill the gap using a deep convolutional network. MR images of 10 healthy subjects (75.5 ± 8.0 years) were retrospectively selected from the Alzheimer's Disease Neuroimaging Initiative database (ADNI). The benchmark of choroid plexus segmentation was provided by the FreeSurfer package and manual correction. A 3D U-Net was developed and optimized in the patch extraction, augmentation, and loss function. In leave-one-out cross-validations, the optimized U-Net provided superior performance compared to the FreeSurfer results (Dice score 0.732 ± 0.046 vs 0.581 ± 0.093 , Jaccard coefficient 0.579 ± 0.057 vs 0.416 ± 0.091 , 95% Hausdorff distance 1.871 ± 0.549 vs 7.257 ± 5.038 , and sensitivity 0.761 ± 0.078 vs 0.539 ± 0.117).

Index Terms— Choroid Plexus, MRI, Segmentation, U-Net, 3D

1. INTRODUCTION

Recent studies show that the cerebrospinal fluid (CSF) flows through the perivascular spaces, which provides a drainage pathway for brain metabolic wastes, including Alzheimer's disease biomarker amyloid-beta [1]. Because the majority of CSF is produced by the choroid plexus, the anatomy and function of the choroid plexus could have an important impact on the CSF production rate and Alzheimer's disease. Therefore, quantitative assessment of the choroid plexus regions is of significant interest.

Several works have reported that the volume of the choroid plexus is associated with certain diseases. Kim et al. reported that the choroid plexus volume is correlated with the Mini-Mental State Examination score in 76 patients with

mild cognitive impairment [2]. Egorova et al. recently reported the enlargement of choroid plexus volume in stroke patients [3]. Zhou et al. found that the volume of the right lateral-ventricle choroid plexus is larger in complex regional pain syndrome patients [4]. Mayinger et al. reported the enlargement of the right choroid plexus in leptomeningeal carcinomatosis patients [5]. However, the measures of choroid plexus volume in the above studies were performed by the atlas-based segmentation of FreeSurfer [6], [7]. The accuracy of segmentation can be improved, as shown in the following sections of this work. The inaccuracy is partly caused by variations in the choroid plexus structure.

Not much research has been reported in choroid plexus segmentation. Although brain segmentation has been studied for decades, the primary focus is the cortical grey matter. In contrast, the choroid plexus region was simply ignored or considered as misclassification regions in ventricle [8] and lesion [9] segmentations. In fetal and neonatal ultrasound images, the choroid plexus regions present outstanding signals. A semi-automatic method was proposed to contour the choroid plexus with a manually selected seed point [10]. The local intensity and regional shape have also been used to train a classifier to identify the choroid plexus regions [11]. Although magnetic resonance imaging (MRI) provides sub-millimeter resolution, a critical challenge of choroid plexus segmentation is the low contrast and the blurred edges, because of the partial volume effect.

Deep convolutional neural networks have been successful in medical image segmentation tasks (e.g. brain tumors, white matter hyperintensities). 3D choroid plexus segmentation experienced seriously imbalanced labels in patch-based approaches. In this work, we optimized a 3D U-Net [12,13] to compensate this issue. The proposed method was compared to FreeSurfer on 10 healthy subjects.

2. METHODS

2.1. MRI scans and Data Description

Data used in the preparation of this article were obtained from the ADNI database (adni.loni.ucla.edu). Consent was obtained and conducted with previous institutes. Deidentified T1-weighted images of 10 healthy female adults (75.5 ± 8.0 years) were retrospectively selected. The

This work was supported by a grant from the Alzheimer's Association (AARF-18-566347), NIH UL1TR001876, NIH U01AG024904, and DOD W81XWH-12-2-0012.

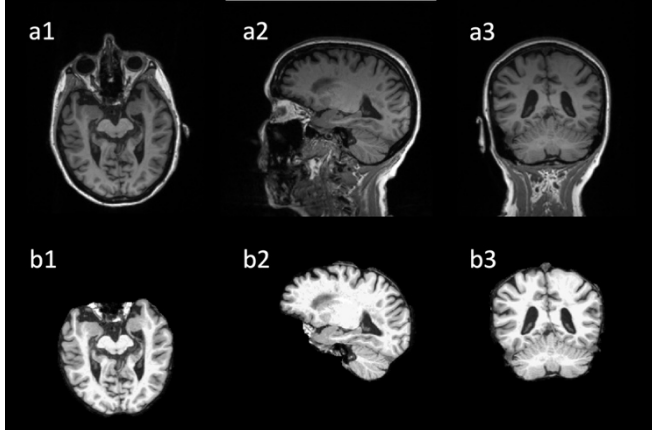


Figure 1 T1-weighted images from a female volunteer at the age of 87. The original images were shown on the top (a) and the preprocessed images were shown on the bottom (b).

images were acquired with accelerated sagittal MPRAGE on a Siemens Prisma 3T Scanner. Inversion time was 900ms, echo time was 2.95ms. TR was 2300ms. Spatial resolution was 1.05mm x 1.05mm x 1.2mm. Flip angle was 9 degrees.

2.2. MRI Scans and Data Description

Because the choroid plexus region is rarely studied in brain anatomy, most segmentation toolboxes or atlases do not provide such regional segmentation. FreeSurfer (Athinoula A. Martinos Center, Boston, MA) was the only published package that can segment the choroid plexus using a brain parcellations pipeline. The standard FreeSurfer pipeline was used here, in which the original images were preprocessed with skull stripping and two normalization steps (the N3 intensity correction on head image and a second intensity correction on the brain region only). The original images and the preprocessed images, Fig. 1, were saved and used as the inputs of the proposed method.

The identified choroid plexus regions in the right and left lateral ventricles were combined with a customized MATLAB script for the following analysis.

2.3. Ground Truth

The choroid plexus segmentation from FreeSurfer was overlaid on the preprocessed image. The choroid plexus regions were manually corrected in three plane view and 3D view using ITK-SNAP [14]. The manually corrected segmentation was considered as ground truth to train the U-Net model and evaluate the performance of the proposed and conventional segmentation methods.

2.4. 3D U-Net Segmentation

The proposed method was modified based on the standard U-Net model. There are two major differences. First, the activation function was chosen as the parametric rectified linear unit (PReLU), which provides extra parameters to

adjust the activation level to achieve improved performance. Second, more features (96) were extracted at the first level of convolution compared to the conventional U-Net.

Each convolution layer was composed of two 3x3x3 kernels. The convolutional features were followed by batch normalization, activation, and a 2x2x2 max-pooling layer. The depth of the encoding and decoding layers was three. At the bottom layer, a dropout rate of 0.5 was used.

The patches were extracted randomly across training subjects with strides 1x1x1. To reduce the inter-patch variance, each T1-weighted image patch was normalized to mean signal 0 and standard deviation 1.

2.5. Label Balances

The choroid plexus region is a small foreground (0.1%) compared to the large background of the brain, which results in imbalanced labels. Because 3D MR images cannot fit in GPU memory, patch-based approaches were explored.

The imbalanced labels could happen inter- and intra-patches, since the choroid plexus region is mainly located at the center of the image. With a small patch size (16x16x16), the average choroid plexus region was 2.3% and the largest choroid plexus region was up to 30%, if a selected patch contained the choroid plexus. Small patch size could reduce the label imbalance within patches. However, 93.5% of the possible patch selections will have no choroid plexus regions. With a large patch size (64x46x64), the intra-patch label balance was low (mean=0.3% and maximum=0.9%) but the majority (96%) of the possible patch selections will have choroid plexus regions.

To handle the inter-patch imbalance, the patches could be extracted according to the probability that if a patch contained more choroid plexus pixels, the patch had a higher probability to be selected for training. In this work, the probability was calculated based on manual corrections of the training patches and was simplified as a linear function that the patch with the maximum choroid plexus regions had the probability of 1 and the patch without the choroid plexus had the probability of 0. This was referred to as nonuniform patch extraction below. As a reference method, the patches were also extracted uniformly but with random orders, which was referred to as uniform patch extraction.

To handle the intra-patch imbalance, a weighted binary cross-entropy was used as the loss function. The choroid plexus and background regions had weights of 0.9 and 0.1.

2.6. Performance Evaluation

The following tests were performed on the preprocessed images: 1) Patch size 16x16x16 vs 64x64x64, 2) uniform vs nonuniform patch extraction, 3) non-augmentation vs augmentation by flipping the brain along left-right direction, and 4) binary cross-entropy vs weighted binary cross-entropy. In addition, 5) the performance on original images and preprocessed images were compared.

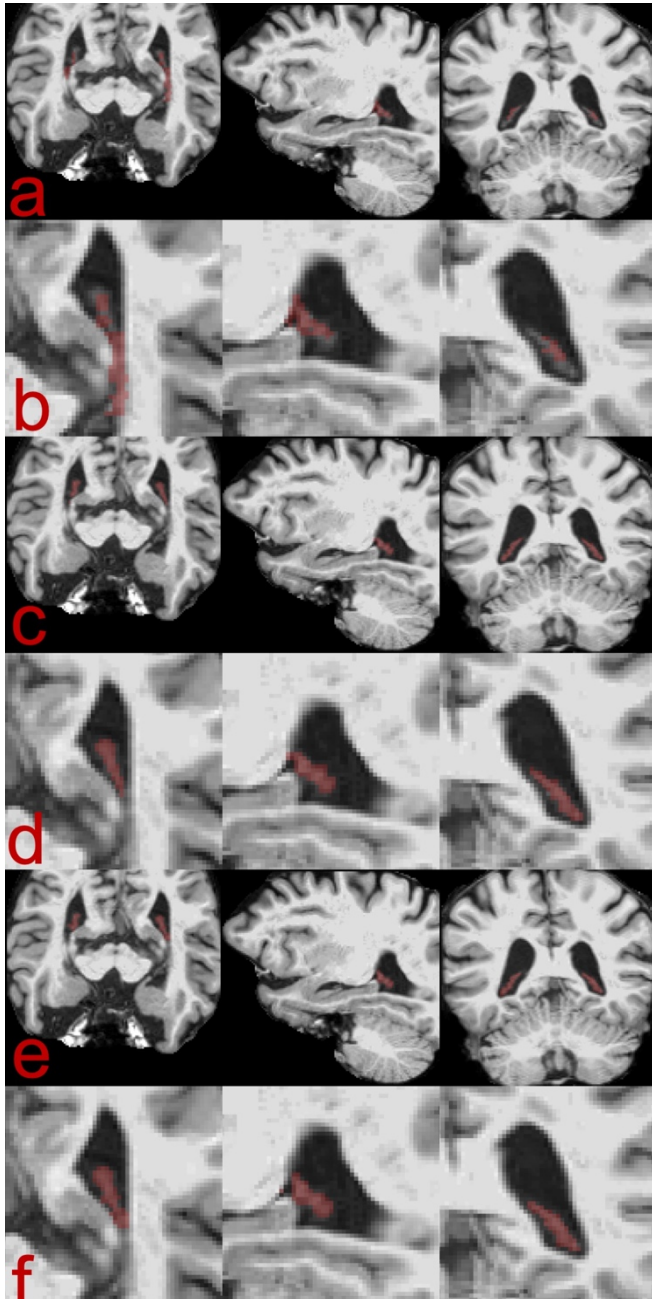


Figure 2 Comparisons of choroid plexus segmentation methods. (a)(b) the FreeSurfer results. (c)(d) the optimized 3D U-Net with preprocessed T1-weighted images. (e)(f) the manual segmentation.

In the training step, other parameters were: Adam optimizer with learning rate 0.0005, 15 epoch, 128 steps per epoch and batch size 4. In the testing step, the labels of the overlapped patches were decided using a majority vote approach, the patch was extracted sequentially with strides of the 1/4 of the patch size. This can ensure that each pixel of the image was voted by the same number of predictions when different patches sizes were used. The proposed

method was implemented in Keras and tested on Nvidia Tesla P100 GPUs.

To fully use the data, leave-one-out cross-validations were performed in each test. The performance of the proposed method was assessed using the Dice score, the 95% Hausdorff distance (95%HD), the sensitivity and the Jaccard coefficient, comparing to the manual correction.

3. RESULTS

Figure 2 shows the choroid plexus segmentation overlaid on the preprocessed brain images. The optimized 3D U-Net (Fig. 2c) produced results that were more consistent with the manual segmentation (Fig. 2e), compared to the FreeSurfer results (Fig. 2a). The differences were more visible in the zoomed images (Fig. 2b, c, and d).

Table 1 top shows the performance metrics of the FreeSurfer results. Compared to the manual segmentation, FreeSurfer resulted in low scores in all the metrics. This may suggest that the choroid plexus volume measurements based on FreeSurfer have limited accuracy. The proposed U-Net methods with a patch size of 64x64x64 resulted in improved performance compared with the FreeSurfer results. More specifically, the optimized U-Net with nonuniform patch extraction, augmentation and weighted binary cross-entropy (weighted_bce) provided the best performance on the preprocessed brain images, highlighted in Table 1.

The patch size of 64x64x64 provided improved results compared to the patch size of 16x16x16. With a small patch size of 16x16x16, the uniform patch extraction failed, which was not shown, and the nonuniform patch extraction showed low accuracy results. The nonuniform patch extraction showed slight improvement with the patch size of 64x64x64.

With argumentation and weighted binary cross-entropy, the proposed method showed sequentially improved results. The proposed method resulted in good performance scores with the original images, but with slightly compromised performance compared to that of the preprocessed images.

4. DISCUSSION

In this work, we developed and optimized a deep convolutional network, the 3D U-Net, for choroid plexus segmentation on MR images. The proposed method outperformed the conventional segmentation provided by FreeSurfer with better Dice, Jaccard, 95% Hausdorff distance and sensitivity scores. The proposed method resulted in slightly reduced performance on the raw MR images, compared to the preprocessed images. This result suggested that 3D U-Net will provide a useful and more accurate tool to assess choroid plexus volume in relative studies.

The proposed method provides an accurate and efficient tool to study the choroid plexus structure.

Table 1 Performance metrics of different methods

		Dice	Jaccard	95%HD	Sensitivity
FreeSurfer		0.581±0.093	0.416±0.091	7.257±5.038	0.539±0.117
U-Net	16x16x16	0.366±0.159	0.237±0.132	51.56±8.296	0.615±0.136
		0.697±0.066	0.538±0.078	2.451±0.944	0.622±0.104
	64x64x64	0.700±0.061	0.541±0.072	2.321±0.783	0.627±0.092
		0.721±0.061	0.567±0.074	2.273±0.938	0.669±0.074
		0.732±0.046	0.579±0.057	1.871±0.549	0.761±0.078
		0.729±0.041	0.575±0.049	2.583±1.563	0.788±0.081

The proposed method showed about 25% higher accuracy in the dice and sensitivity scores, compared to the atlas-based segmentation provided by the FreeSurfer, and it will provide reliable quantification of the choroid plexus volume and reliable locations of the choroid plexus for regional analysis.

The proposed method showed better performance with preprocessed images, compared to the original images. The preprocessing step reduced the spatial variances between subjects by intensity normalization and removed the unrelated structures, such as the skull, which reduced the noise in the data. The performance of the proposed method was slightly reduced with the original data, which is still largely improved compared to the conventional method. In the studies with a large number of subjects, direct segmentation on the original image could be feasible, although further evaluation is needed.

Although a small patch size has a better inter-patch balance, it brought up two problems. First, the imbalance among patches was serious, which may directly cause the failure with uniform patch extraction. Second, with nonuniform patch extraction, the small patch size resulted in a low accuracy in the segmentation. This is partly because the small patch focused on the local structure, which mislabeled other ‘belt’ structures in the brain as the choroid plexus region. In contrast, a large patch size provided more stable and high accuracy results.

This study had several limitations. First, this study included a small cohort. Although the model was trained on extracted patches with large sample size, the robustness of the proposed method requires further evaluation with a large cohort. Second, the current study focused on the choroid plexus in the lateral ventricle. This region was selected partly because it has been pre-labeled in the FreeSurfer result and because these are also the most recognizable regions in the manual segmentation. Third, the depth and the number of features could be optimized further for each patch size to achieve the best performance. Fourth, other loss functions (e.g. dice loss) could be explored for additional performance improvement.

In conclusion, our work demonstrated the feasibility and the superior performance of the 3D U-Net method for choroid plexus segmentation, compared with an atlas-based segmentation method. This method provides an efficient tool to measure the choroid plexus quantitatively. Its improved accuracy can provide reliable measurements in

related pathology studies with a large cohort. Future work will investigate the choroid plexus volume of AD patients.

5. REFERENCES

- [1] J. J. Iliff et al., “Cerebral Arterial Pulsation Drives Paravascular CSF-Interstitial Fluid Exchange in the Murine Brain,” *J. Neurosci.*, vol. 33, no. 46, pp. 18190–18199, 2013.
- [2] G. E. Kim et al., “Choroid Plexus Volume Is Associated With Cognitive Function in Late Life,” *Alzheimer’s Dement.*, vol. 14, no. 7, p. 856, 2018.
- [3] N. Egorova, E. Gottlieb, M. S. Khelif, N. J. Spratt, and A. Brodtmann, “Choroid plexus volume after stroke,” *Int. J. Stroke*, vol. 0, no. 0, pp. 1–8, 2019.
- [4] G. Zhou, J. Hotta, M. K. Lehtinen, N. Forss, and R. Hari, “Enlargement of choroid plexus in complex regional pain syndrome,” *Sci. Rep.*, vol. 5, pp. 1–5, 2015.
- [5] M. Mayinger et al., “MRI based neuroanatomical segmentation in breast cancer patients: leptomeningeal carcinomatosis vs. oligometastatic brain disease vs. multimetastatic brain disease,” pp. 1–7, 2019.
- [6] B. Fischl et al., “Whole Brain Segmentation: Automated Labeling of Neuroanatomical Structures in the Human Brain,” *Neuron*, vol. 33, no. 3, pp. 341–355, 2002.
- [7] B. Fischl et al., “Automatically Parcellating the Human Cerebral Cortex,” *Cereb. Cortex*, vol. 14, no. 1, pp. 11–22, 2004.
- [8] Y. Wu, K. Pohl, S. Warfield, and C. CRG, “Automated Segmentation of Cerebral Ventricular Compartments,” vol. 13, p. 2115, 2002.
- [9] B. J. Bedell and P. A. Narayana, “Automatic segmentation of gadolinium-enhanced multiple sclerosis lesions,” *Magn. Reson. Med.*, vol. 39, no. 6, pp. 935–940, 1998.
- [10] B. Sciolla, M. Martin, P. Delachartre, and P. Quetin, “Segmentation of the lateral ventricles in 3D ultrasound images of the brain in neonates,” *IEEE Int. Ultrason. Symp. IUS*, vol. 2016-Novem, pp. 1–4, 2016.
- [11] R. Huang, A. Namburete, and A. Noble, “Learning to segment key clinical anatomical structures in fetal neurosonography informed by a region-based descriptor,” *J. Med. Imaging*, vol. 5, no. 01, p. 1, 2018.
- [12] O. Ronneberger, P. Fischer, and T. Brox, “U-Net: Convolutional Networks for Biomedical Image Segmentation,” *arXiv:1505.04597*, pp. 1–8, 2015.
- [13] Ö. Çiçek et al., “3D U-Net: Learning Dense Volumetric Segmentation from Sparse Annotation,” *MICCAI*, pp. 424–432, 2016.
- [14] P. A. Yushkevich et al., “User-guided 3D active contour segmentation of anatomical structures: Significantly improved efficiency and reliability,” *Neuroimage*, vol. 31, no. 3, pp. 1116–1128, Jul. 2006.